Experimental Investigation on Solar-Driven GAX-based Absorption Heat pump for Domestic Hot Water production

Hai Trieu Phan, Fabio Aste and Hélène Demasles

Université Grenoble Alpes, CEA, Liten, Campus INES, 73375 Le Bourget du Lac, France

Abstract

This paper presents a new development of NH_3-H_2O absorption heat pump designed with plate heat exchangers and market ready components in order to offer a compact machine easy-to-manufacture. An innovative architecture based on GAX (Generator Absorber Heat Exchange) cycle has been proposed for an optimal use of the internal heat of the cycle for absorption and desorption processes. A model has been built for design of a prototype with the production target of 25 kW of hot water (> 60°C) from a lower-temperature heat source of around 30°C. The prototype has been tested under various conditions. The thermal Coefficient Of Performance (COP) and the electrical coefficient of performance (ECOP) obtained at nominal conditions are respectively 1.52 and 130. Furthermore, the machine shows its capacity to operate over a wide conditions range, especially in term of the inlet temperature of the heat source from 110°C to 170°C.

Keywords: Absorption heat pump, Ammonia/water, GAX, prototype

Nomenclature

			Subscripts	
C_P	Specific heat	[J/kg.K]	A	Absorber
DX	Concentration difference between rich and poor solution	[-]	abs	absorption
DT	Temperature glide	[K]	C	Condenser
E_K	Kinetic energy	[J]	des	desorption
E_Z	Potential energy	[J]	el	electric
h	Enthalpy	[J/kg]	E	Evaporator
$\dot{m}$	Mass flow	[kg/s]	G	Generator
P	Pressure	[bar]	in	input
Q	Heat exchange rate	[W]	m	motor
T	Temperature	[K]	out	output
x	Ammonia concentration	[-]	sat	saturation
W	Work	[W]	sp	poor solution
			sr	rich solution
Acronyms			v	vapour
COP	Coefficient Of Performance	[-]	w	water
ECOP	Electrical coefficient of performance	[-]		

1. Introduction

In France, the residential and industrial sectors account for 23Mtoe of electric consumption, while the natural gas consumption attests on 24Mtoe (IEA database). In general, these two sectors are responsible of the 43.2% of the French total final consumption, and a great part of this share is converted into heat. In the residential sector, the 78% of the consumption is dedicated to space heating and cooling through systems that are fed for 58% with fossil fuels (https://www.ceren.fr/). Industry is as well dependent on fossil fuels (61% of the total consumption) for heat generation, with even a small share of the electricity consumption (18%, i.e. 21 TWh in 2013) used for thermal production. During the processes, about the 25-60% of the heat is lost to the environment, for a total amount of 8.56 Mtoe of waste heat (https://www.ademe.fr/). However, this rejected heat is available at different temperature levels: almost a third is available at >100°C and can be re-used on site

doi:10.18086/eurosun.2022.08.10 Available at http://proceedings.ises.org

or for feeding heating networks; the second third, between 40°C and 100°C, can be enhanced in temperature by heat pumps; the remaining third is rejected at a temperature < 40°C and is hardly exploitable. The challenge is saving the medium-and-low-temperature heat from being wasted, increasing the overall process performance and reducing the Greenhouse Gas (GHG) emissions. In this context, one of the most adapted solutions is represented by the absorption heat pumps, which use natural fluids and allow upgrading low-temperature sources to a higher temperature level using heat as fuelling. In addition, such systems can also be configured in reverse mode to produce cooling, addressing both industrial and residential needs.

To operate, absorption machines need a heat source that can be indifferently gas, renewable heat (solar, geothermal, biomass) or waste heat, with an increased economical end environmental interest in the two last cases. Concerning heating, absorption heat pumps can effectively contribute to lower the global energy consumption for both residential and industrial sectors, thus reducing the GHG emissions in accordance with the European Energy-Climate Framework 2030 and the international goals for limiting the global warming.

As absorption cycles require two fluids for operating, refrigerant and solvent, many possibilities of coupling exist in the literature according to Sun J. et al. (2012). The most diffused are ammonia-water and water-lithium bromide due to their interesting thermophysical properties. This last couple has historically been chosen for air conditioning, and in the last decades, it found application even in some heat pumps [Aprile M. et al. (2016), Dai E. et al. (2018) and Wang J. et al. (2019)]. Despite its good efficiency, especially in multi-stage systems, H_2O/LiBr has two important drawbacks: a limited operating field, by both crystallization risk and water freezing temperature, and an important cost. Ammonia-water couple avoids these problems, being suitable to operate in large temperature fields and having a lower cost, as ammonia is a common product. For the pursuit of the work, NH_3/H_2O will be the chosen fluid couple.

Amongst the different ammonia-water absorption cycles, the Generator-Absorber heat eXchanger (GAX) cycle is the most interesting due to its flexibility and increased performance compared to the single stage cycle. This cycle can effectively operated as a chiller, down to -40°C, or as a heat pump, even above 70°C with high efficiency. Despite that, few GAX heat pumps exist on the market and most of them base on expensive and bulky heat exchangers in the form of distillation columns.

According to the literature, Aprile M. et al. (2016) tested an industrial gas-driven, GAX heat pump that produces 20 kW of hot water at 60°C or 45°C (evaporator temperature $T_{E,in}$=10°C) with Coefficient of Performances (COP) of 1.6 and 1.73 respectively. Dai E. et al. (2018) tested an industrial 55 kW absorption heat pump that can produce 55°C hot water with an optimal COP of 1.63 at $T_{E,in}$=20°C and generator temperature $T_{G,in}$=200°C. The other heat pump present in the literature is a prototype made by Wang J. et al. (2019), where the main heat exchangers consist in tailored-made shells-and-tubes exchangers, thus not compact. The best performance obtained is COP = 1.51 with $T_{E,in}$=15°C and $T_{G,in}$=193°C. According to these works, the development of GAX heat pumps is particularly interesting for high-temperature waste heat recovery and, due to the COPs above 1.5, even the case of fuelling with fossil sources (gas, biomass, etc.) becomes environmentally and economically attractive.

In this paper, a novel GAX architecture is presented, together with the related numerical model. The prototype is designed, fabricated and tested according to this architecture using only commercially available components, such as plate-type heat exchangers in order to improve the compactness, the amount of charge (ammonia) as well as the minimize the constraint related to high pressure. During the experimental investigations in the laboratory test rig, a particular attention has been given to the operating conditions, which have been varied to test the response of the system in different situations. The experimental results are then discussed to analyse the impact of the main parameters, such as the generator temperature, the evaporator temperature and the solution flow rate.

2. Cycle description

As introduced before, NH3/H2O is chosen for the study due to its favourable properties. In addition, this fluid couple is particularly interesting from an industrial point of view, being ammonia a well-known element used in plenty of domains, thus largely available and cheap. In this sense, the components of the GAX heat pump

that is further proposed are chosen amongst commercial parts, as plate heat exchangers and pressurized tanks, to demonstrate the viability of such absorption systems.

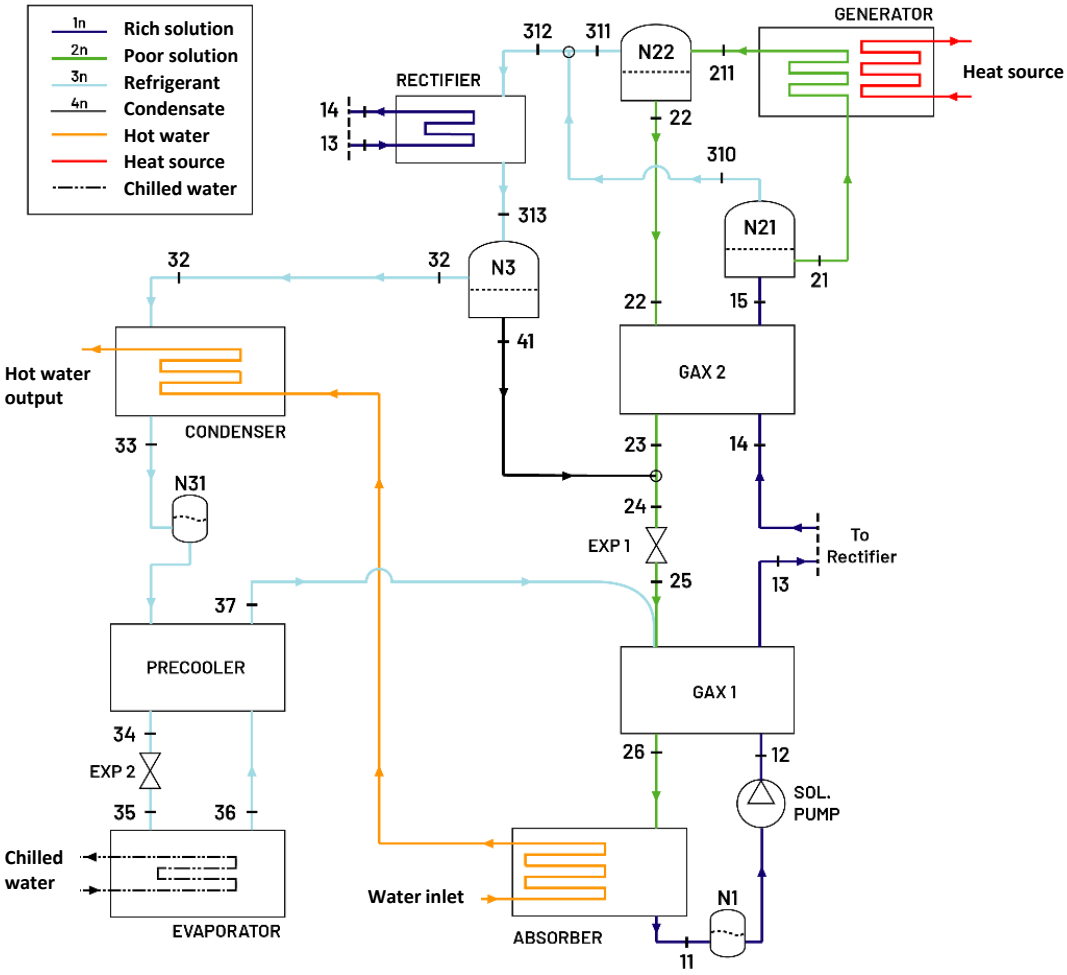

Figure 1: Scheme of GAX prototype architecture

Detailing the architecture, the GAX heat pump cycle shown in Figure 1 features a novel architecture where the vapour generation process is discretized via different components, three heat exchangers (GAX2, generator and rectifier) and three pressurized tanks (N21, N22 and N3). This approach is quite the opposite of the standard one, which involves a single element for both heat and mass transfers. A similar case can be made about the absorber too.

2.1 Working principle

As this study concerns a heat pump, the absorber and the condenser are cooled in series to maximise the cooling fluid output temperature. After preliminary simulations, the cycle is found to perform better if the absorber is entered first. In heat pump mode, the useful effect consists in the heat delivered to the cooling fluid, while the high-temperature heat entering the generator acts as the driving power. The heat flux entering the evaporator is seen as a free input.

For a convenient description, the heat pump cycle is roughly divided into three subcycles according to the different fluids: refrigerant, rich solution and poor solution.

- Refrigerant subcycle

Rich solution diphase flows coming from GAX2 and generator enter the two separation tanks N21 and N22 respectively: there, the vapour separates by gravity from the liquid solution. Due to the difference in the saturation pressures, the liquid is richer in water and the vapour is richer in ammonia, but it is generally not pure. Therefore, the vapour is sent to the rectifier to be enriched in ammonia. The purification occurs through

the refrigerant cooling, which causes a partial condensation of the fluid: the water-rich condensate is recirculated to the poor solution line. In parallel, the purified refrigerant is firstly condensed, then subcooled in the precooler before throttling, and finally vaporized in evaporator. After that, the vaporous refrigerant flows through the low-pressure side of the precooler and reaches the GAX1, where the absorption reaction with the poor solution begins.

- Rich solution subcycle

The rich solution is obtained as the product of the absorption reaction, which begins in the GAX1 and ends in the absorber. There, the ammonia-water mixture presents the highest richness in ammonia and its thermodynamic state is subcooled liquid, which allows protecting the pump. This last component increases the pressure of the rich solution that is subsequently delivered to the GAX1 (12) to be warmed. In this first heating phase, desorption might already occur. The desorption process continues in the rectifier and in the GAX2, as the rich solution recovers the available internal heat of the other fluid lines. Being diphasic after the GAX2, a first phase separation is performed in the N21 tank to avoid sending some vapour in generator inlet. Here, the remaining rich solution is heated to the highest temperature to continue desorption process. The two-phase fluid undergoes a second and final phase separation in the N22 tank, resulting in the poor solution and some additional refrigerant vapour at the outlets.

- Poor solution subcycle

After phase separation in the N22 tank, the poor solution features the lowest richness in ammonia in the cycle and the highest temperature too. A first heat recovery occurs towards the rich solution in the GAX2. Then, the poor solution is mixed with the condensate, increasing ammonia richness and decreasing the temperature. The resulting solution is throttled before entering the GAX 1 (25). There, the ammonia vapour coming from the refrigerant subcycle (37) is absorbed by the poor solution and, as the absorption reaction is exothermic, heat generation occurs. The internal recovery is realized by the rich solution (13). The complete absorption in GAX1 is limited by the temperature level of the rich solution used for the cooling. Thus, the reaction is continued in the absorber where further absorption is done by cooling with a colder external source.

- GAX effect

The GAX cycle is particularly interesting when a large temperature overlap between the generator and absorber occurs: in this case, absorption excess heat is partially available at a temperature that allows the rich solution desorption in GAX1. In GAX2 and rectifier, the desorption continues thanks to the internal heat recovery from the poor solution. Taking advantage of this temperature overlap decreases the input heat in the absorber and the generator, improving the global performance and reducing the absorber and generator components size.

2.2 Comparison with literature architectures

Only little experimental work has been done on GAX systems configured as heat pumps. Aprile M. et al. (2016) tested an absorption heat pump manufactured by the Robur Company in Germany, Dai E. et al. (2018) tested one manufactured by the Vicot Company in China, and only Wang J. et al. (2019) tested a self-made prototype.

The main difference between the proposed architecture and the existing ones consists in the vapour generation system and the absorption system. An immediate finding can be made about the rich solution circuit, which shows a different path: instead flowing first through the rectifier and then through the GAX, in the proposed version it encounters first the GAX1, then the rectifier, and finally the GAX2. This variation results from the pinch analysis of the system fluid lines and optimizes the internal heat recovery.

A more technical aspect concerns the heat exchangers technology. In the literature, the technologies used for the components where absorption takes place (GAX1 and absorber) vary according to the authors : two separated falling film heat exchangers tubes in tubes type [Aprile M. et al. (2016) and Wang J. et al. (2019)] or shell-and-tubes exchangers, which allows piling the two units to form a single component [Dai E. et al. (2018)]. However, all authors choose the same technology for the desorption block : Generator, GAX2 and rectifier are shell-and-tubes exchangers, which allows piling the three units where the ammonia vapour flows in counter-current respect to the solution, being cooled and rectified all along as in a distillation tower. Therefore, the refrigerant vapour is already purified when exiting the generation column and the condensate resulting from rectification is directly recirculated in the underlying sections. Since the vapour generation and

separation occur simultaneously, the generation block is sized taking into account the two process. The novel architecture proposed in this work avoids dealing with this point: as the heat and mass transfers and the phase separation occur separately, each component is optimally sized to its function.

Another aspect to be considered is the system manufacturing. Generally, these distillation-column-like elements consist in a cylindrical vessel where the different sections are heated or cooled by coil exchangers. Such assembly requires a complex manufacturing and, due to the low heat transfer coefficient of coil exchangers, it presents a considerable volume that cannot be split without losing all the advantages of a coupled vapour generation and separation. Differently, the proposed architecture involves many smaller units that can be distributed in the space, thus allowing a more rational positioning inside the system and an easy maintenance.

3. Modelling approach

To determine the most efficient solution for the novel GAX ammonia-water cycle, many architectures have been modelled and then implemented in the software EES (Engineer Equation Solver, http://www.fchart.com/) to be numerically studied. EES internally provides NH_3/H_2O mixture thermodynamic properties, which are calculated through the correlations proposed by Ibrahim O.M. and Klein S.A. (1993). By specifying the heat and mass efficiencies of the components and integrating the hypothesis listed in Table 1, the model returns the thermodynamic conditions of the state points of the cycle and the global performances.

Table 1: Hypothesis of the model for the prototype design

The system is at steady state;	Adiabatic components and pipes;
ΔE_K and ΔE_Z are negligible	Ideal heat sources and sinks;
Pressure drops are negligible;	Pump has $\eta_{el} = 0.9$ and $\eta_m = 0.8$;
Saturated fluid at separation tanks outlet;	The heat transfer efficiency is 0.8;
The approach temperature in heat exchangers is 5°C;	Absorption efficiency is 0.8 and desorption efficiency is 1 according to Boudehenn F. et al. (2014);
Evaporator temperature glide is 5°C;	

The model is established considering each component as a control volume, thus is 0D: the internal dynamics are excluded from the study, as the behaviour of the component is considered as a whole and included in the relative efficiency. Even if simple, this approach is reliable for the scope, as it has been largely demonstrated in previous works [Herold K. E. et al. 1996].

For each control volume, mass and energy conservation equations have been defined:

$$Total\ mass\ conservation \rightarrow \sum \dot{m}_{in} - \sum \dot{m}_{out} = 0 \quad \text{Eq. 1}$$

$$Refrigerant\ mass\ conservation \rightarrow \sum \dot{m}_{in}\, x_{in} - \sum \dot{m}_{out}\, x_{out} = 0 \quad \text{Eq. 2}$$

$$Energy\ conservation \rightarrow \sum \dot{m}_{in}\, h_{in} - \sum \dot{m}_{out}\, h_{out} + \sum \dot{Q} - \sum \dot{W} = 0 \quad \text{Eq. 3}$$

In the last equation, Q and W are the heat and work fluxes exiting the system boundary. Signs respect the traditional convention.

The evaporator temperature glide is defined as $T_{36} - T_{35}$.

Finally, the Coefficient Of Performance (COP) of a generic heat pump is defined as the ratio between the heat rejected to the external cooling fluid at the condenser and the energy input in the compressor. In the case of absorption cycles, a heat rejection occurs also in the absorber, as the absorption reaction is exothermic. This heat being recuperated by the external cooling fluid, it becomes a part of the useful effect. The energy input

changes too: in fact, besides the electric energy consumption, an additional and more consistent high-temperature heat consumption is necessary to power the system. Generally, it is good practice to distinguish the type of COP between electrical (ECOP) and thermal (COP) for the continuation, as heat consumption largely prevails on the electric). In particular, doing techno-economic analysis one of the two parameters is often negligible while the other drives the decision.

$$Electrical\ Coefficient\ Of\ Performance \rightarrow ECOP = \frac{\text{useful energy}}{\text{electric cost}} = \frac{\mathrm{Q_A} + Q_C}{\mathrm{W_{el,pump}}} \quad \text{Eq. 4}$$

$$Thermal\ Coefficient\ Of\ Performance \rightarrow COP = \frac{\text{useful energy}}{\text{heat cost}} = \frac{\mathrm{Q_A} + Q_C}{Q_G} \quad \text{Eq. 5}$$

According to simulations, the best performance considering both COP and ECOP is obtained for the architecture given in Figure 1. This model has also been used to size all the components of the prototype.

4. Experimental system

4.1 Prototype

The sizing conditions are reported in Table 2. The generator inlet temperature is set at 170°C, corresponding to the optimal numerical COP. The target of the machine is to produce 25 kW of hot water (> 60°C) from a lower-temperature heat source (~ 30°C).

Table 2: Prototype sizing point

Parameters	Value	Measure Unit
Generator inlet temperature	170	°C
Absorber inlet temperature	30	°C
Evaporator inlet temperature	35	°C
Target hot fluid outlet temperature	> 60	°C
Target heating capacity	25	kW

Using these values as model inputs, the characteristic parameters of the components have been defined. Then, each element has been identified on the market, purchased and assembled. To respect the technological readiness asset, only industrial brazed/welded plates heat exchangers are implemented, as those last components are standardized and produced in series. Instead, the piping and separation tanks, even if they are well known industrial elements, must be designed and singularly manufactured to fit the operating conditions. In addition, as the ammonia/water mixture is very corrosive, a special care is taken by selecting only resistant components, mostly made in stainless steel. Considering the material costs of the assembly without instrumentation, the pressurized tanks (36%) and the piping (25%) represent a great share, while the plate heat exchangers affect for a littler amount (13%). A picture of the prototype is shown in Figure 2.

Three stainless steel tanks are used to separate refrigerant vapour and liquid solution at the outputs of generator, GAX2 and rectifier. Two other tanks are provided as fluid storages: one to store the poor solution before pumping, in order to avoid pump cavitation during the start-up phase; the other one to store the refrigerant after the condenser. These two last tanks allow the heat pump to be operated over a wide temperature range. However, the system is filled with relatively low quantities of water and ammonia, 1.4 kg of water and 2.4 kg of ammonia. Finally, the GAX1 heat exchanger features an original, double distributor system for the poor solution and refrigerant inlet, allowing liquid and gas flows to be uniformly distributed into each channel.

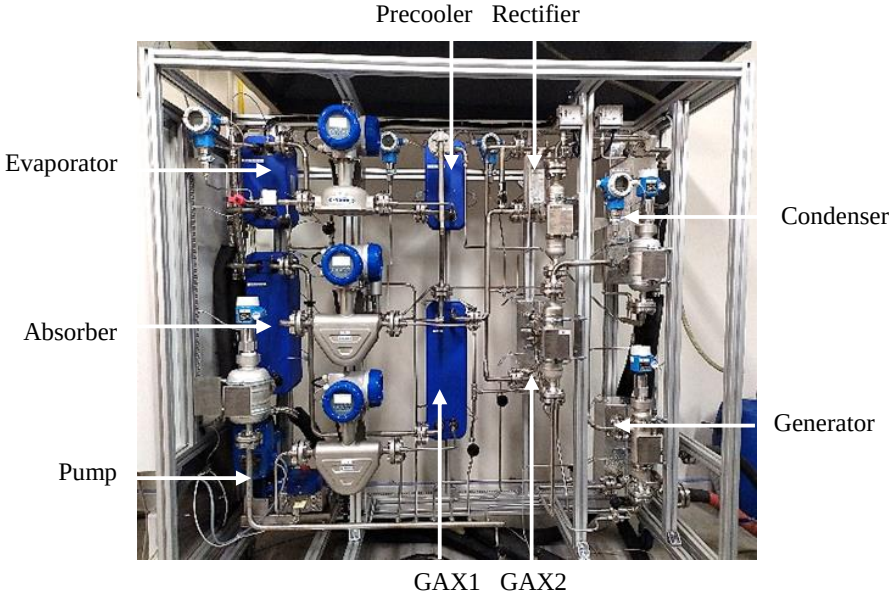

Figure 2: Front view of the GAX prototype

4.2 Characterization

Experimental tests were performed at the INES (French National Institute for Solar Energy) facility in a test rig that allowed providing adjustable temperatures and powers for the external fluids. The fluid chosen for all external circuits is pressurized water. The heat pump operating field during the tests is reported in Table 3.

Table 3: GAX heat pump operating range during experimental test. Data refers to external-side fluid for Evaporator, Absorber, Condenser and Generator and to the internal-side fluid (rich solution) for the Pump. In the case of the Pump, both upstream and downstream pressures are indicated.

		Evaporator	Absorber	Condenser	Generator	Pump
Inlet temperature [°C]	Nominal	34.6	29.5		170	41
	Minimal	25	29.5		110	35
	Maximal	50	29.5		170	47
Pressure [bar]	Nominal	9	10.5	23.4	23.6	10.5/23.6
	Minimal	7.5	7.5	19	19	7.5/19
	Maximal	13	13	24	24	13/24
Power [kW]	Maximal	13.4	16	14.6	18.9	0.2
Mass flow rate [kg/h]	Minimal	1700	320	320	950	
	Maximal		865	865		

4.3 Measurement apparatus

The prototype is instrumented with high-precision sensors in order to measure the parameters needed for a thorough comprehension of its functioning. Temperature sensors are positioned on the heat exchangers inlet/outlet. Pressure sensors are positioned on the high- and low-pressure solution and refrigerant circuits. Coriolis flowmeters are employed to measure mass flow, density and temperature of the internal fluids. Liquid level sensors are placed inside the pressurized tanks to measure the amount of the stocked liquid, thus describing the fluid distribution in the prototype. In addition, the level sensor in the storage tank upstream the pump has a protection function, as it shuts off the pump when the stocked liquid level is too low.

Type and uncertainty of the instrumentation are described in Table 4.

Table 4: Instrumentation characteristics

Parameters	Sensors type	Quantity	Uncertainty (+/-)

Heat transfer fluid temperature	Pt100	8	0.1 K
Refrigerant/Solution temperatures	Thermocouples	25	0.3 K
Refrigerant/Solution pressure	0-10 bar and 0-40 bar	4	0.2% full scale
Refrigerant/Solution flow	Mass flowmeter	3	0.20%
External fluid flow	Mass flowmeter	4	0.30%
Density	Mass flowmeter	3	2 kg/m^3
Liquid level	Capacitance level sensor	3	0.50%

4.4 Data processing

Despite the number of sensors deployed across the system, many parameters cannot be directly measured and need to be calculated afterwards. In particular, it is the case of the flow rates in the poor solution and condensate lines, and the heat fluxes in the heat exchangers. The firsts are determined through total mass and refrigerant mass balances; the lasts require energy balances in addition. The heat flux can be properly calculated only on absorber, generator, condenser and evaporator where the measures are accurately done on external fluid. As an example, the absorber heat flux is defined:

$$Q_A = \dot{m}_A c_{P,w}\left(T_{A,out} - T_{A,in}\right) \quad \text{Eq. 6}$$

Where $C_{P,w}$ is the specific heat of water and $\dot{M}$ is the heat carrier fluid flow. However, on internal heat exchangers where there are absorption or desorption reactions, the heat flux cannot be calculated as it is impossible to know the enthalpy of the fluid precisely.

4.5 NH_3 concentration

Determining the ammonia concentration of the solution is an essential point to qualify the functioning of the system. Therefore, ammonia fractions are calculated from measured density, temperature and pressure through reverse correlations based on Ibrahim O.M. and Klein S.A. (1993). The maximum error is ±2.5%.

5. Experimental results

5.1 Performance comparison to state-of-the-art systems

To facilitate the comparison of absorption chillers performances, the COP is generally showed in relation to the Carnot COP, a conventional parameter that characterizes the operating conditions of the system. The definition of the Carnot COP can be found in the literature [Boudehenn F. et al. (2014)]. This same logic can be applied to heat pumps, although a modification of the formulation is required.

On the presented prototype, the useful effect occurs throughout the absorber and the condenser as the absorption and condensation heat is released to the external fluid, which heats up to the $T_{AC,out}$ temperature. Considering the heat fluxes, the First Law of Thermodynamics gives:

$$Q_G + Q_E + Q_{(A+C)} = W \quad \text{Eq. 7}$$

With the mechanical work provided by the pump being negligible compared to the energy fluxes. Then, under the hypothesis of cycle reversibility, the Second Law Thermodynamics can be written as:

$$\frac{Q_G}{T_{G,in}} + \frac{Q_E}{T_{E,in}} + \frac{Q_{(A+C)}}{T_{AC,out}} = 0 \quad \text{Eq. 8}$$

Where $T_{AC,out}$ represents the temperature of the useful heat production, $T_{G,in}$ represents the high-temperature heat source that feeds the generator and $T_{E,in}$ represents the low-temperature heat source that interfaces with the evaporator. From Eq. 16 and Eq. 17, the Carnot COP for heat pumps can be derived as:

$$COP_{Carnot} = \frac{T_{G,in} - T_{E,in}}{T_{G,in}} \cdot \frac{T_{AC,out}}{T_{AC,out} - T_{E,in}} \quad \text{Eq. 9}$$

In Figure 3, the experimental COPs of the presented prototype and other different GAX heat pumps are reported for comparison, giving an overview of the ammonia-water heat pumps global panorama. The current work prototype shows the same performance of Wang J. et al. (2019)'s prototype. Better performances are obtained by Aprile M. et al. (2016) and Dai E. et al. (2018), which have both chosen commercial systems for their studies.

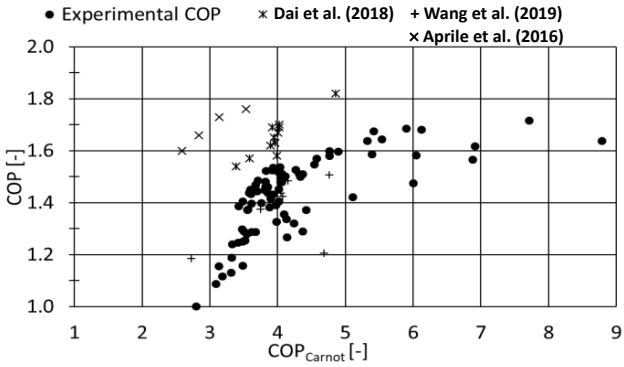

Figure 3: Comparison of thermal COP as function of the Carnot efficiency

Some general considerations can be done about the working fields of the presented systems. Dai E. et al. (2018) concentrate in a narrow area corresponding to a precise Carnot COP, varying their performance mainly depending on the absorber inlet temperature. Instead, Wang J. et al. (2019) and Aprile M. et al. (2016) systems cover a wider area, with COP trends that seem reaching a plateau after a certain Carnot COP. The current work shows a significantly large Carnot COP field, with average performances higher than Wang's et al. prototype and maximum COP in line with Dai E. et al. (2019)'s results.

Finally, observing the point distribution, a denser area is visible at Carnot COP next to 4.0. Many tests have been performed around this condition as it coincides with the sizing point of the system. The rest of the measured points are relatively scattered, which is due to working in a wide field of solution flow rates and temperatures. A summary of the operating conditions and the performances at the nominal point and at the maximum-power point is reported in Table 5.

Table 5 : Operation conditions and performances at the nominal and maximum-power points

	$T_{E,in}$	$T_{A,in}$	$T_{G,in}$	$T_{C,out}$	M_{12}	Q_G	Q_{A+C}	COP	COP_{Carnot}
Nominal	35	30	170	60	100	16	25	1.52	4.0
Max Q_{C+A}	49.4	29.3	150	60	113	18.6	32	1.72	7.7

5.2 Comparison at nominal conditions

A focus on the performance at sizing conditions is reported in Figure 4. The generator, evaporator and absorber inlet temperatures are respectively 170°C, 35°C and 29.5°C, while the outlet target temperature is 60°C. To attend this value, the absorber and condenser external fluid flowrates are varied between 570 kg/h and 700 kg/h. Instead, the external flow rates in generator and evaporator are kept constant at respectively 950 kg/h and 1700 kg/h to guarantee a proper temperature pinch. The rich solution flowrate is approximately 100 kg/h. As the average useful heat power produced in the absorber/condenser is 23.7 kW (13.6/10.1 kW), and as the average heat input in the generator is 15.6 kW, then the resulting COP is 1.52.

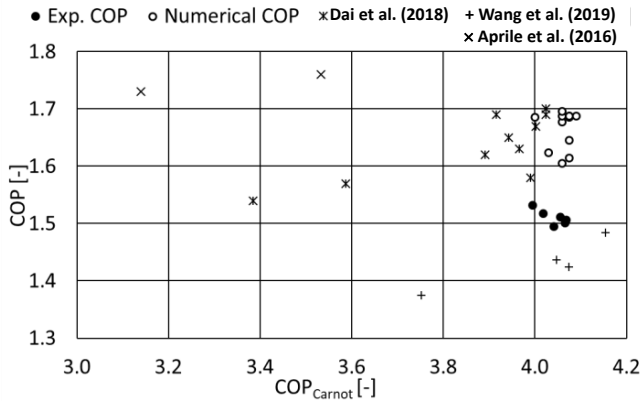

Figure 4: Numerical and experimental COP as function of the Carnot efficiency with focus on the prototype nominal conditions

Figure 4 allows comparing the numerical COP obtained from the numerical model with the experimental observations. In general, the measured performances are 10% lower than the simulated values. This might be due to different reasons: an improper configuration of the absorber, constraints in the prototype operation due to a limited thermo-mechanical resistance of the components and a reduced control of the rectification in some operating conditions. Nevertheless, if the numerical performances are in line to those of Dai E. et al. (2018), they remain lower than those of Aprile M. et al. (2016). A possible explication can be found in the technology chosen for the vapour generation. Both literature authors utilise tubes-and-shell exchangers, because this solution allows different sections to be stacked together creating a single exchange volume where refrigerant vapour and liquid solution are in counter-current, which favours heat and mass transfers. Instead, the adoption of plate heat exchanger technology allows having a more compact and easy-to-manufacture system, but with a lower mass transfer efficiency. Aste F. and Phan H.T. (2022) numerically compared these two technologies and observed that there is an impact of up to 20% in the COP for GAX systems. An interesting compromise has been introduced by Wirtz M. et al. (2021), who proposed a plate heat exchanger where the generation and rectification sections are stacked. This concept takes advantage of the refrigerant vapour and liquid solution counter-current flow, yet remaining compact.

5.3 Effects of operating conditions

As the experimental campaign was carried through the conditions reported in Table 3, the impact of different parameters on the system performance has been evaluated. In particular, the study concerns the influences of the solution flowrate, the generator temperature and the evaporator temperature.

Some preliminary observations can be presented with reference to Figure 5. The target temperature for the hot water production ($T_{C,out}$=60°C) is reached for most points, despite the wide field of working conditions. Moreover, the hot water outlet temperature seems being stable at different system heat duty (from -50% to +30% nominal power), meaning that off-design operation is feasible.

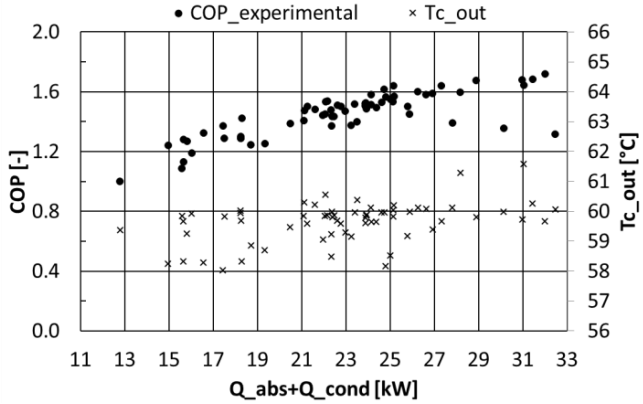

Figure 5 : COP and the outlet hot water temperature as functions of the heating capacity

Nevertheless, the COP strongly depends on the operating conditions, which reflect onto the absorber and condenser heat duties, with a sharp decrease below the nominal value (25 kW). Besides, in Figure 6 the ECOP has an almost linear tendency with reference to the increase of the useful heat production Q_A+Q_C. The highest heating power, 33kW, the best COP of 1.72 and the best ECOP of 170, are reached at 150°C, 30°C and 49.4°C respectively as generator, absorber and evaporator inlet temperatures.

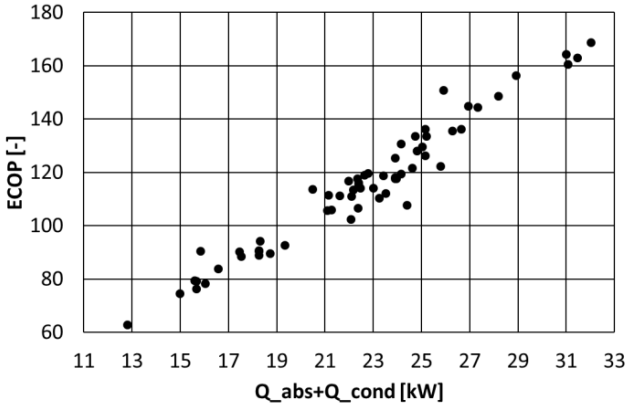

Figure 6 : Electrical COP (ECOP) as a function of the heating capacity

- Rich solution flow variation

The impact of rich solution flow rate ($\dot{m}_{12}$) is studied at the nominal temperatures of $T_{a,in}$=29.4°C, $T_{g,in}$=169.8°C and $T_{e,in}$= 34.5°C. Figure 7(a) shows that an increase in the rich solution flow rate leads to an increase in powers output of all heat exchangers, except for the evaporator. Despite the augmentation in the refrigerant vapour flow $\dot{m}_{32,}$ its exchanged heat does not follow the same trend. The evaporator appears to be limited by its size, since a decrease of the temperature glide is observed, as shown in Figure 7(b), even when a control target is set at 5K. In addition, we observed that the increase of the exchanged power in the absorber is smoother than in the generator (Figure 7(a)). A possible explanation is that the mass transfer by absorption process in GAX1 and in the absorber deteriorates with an increase of liquid fraction at the outlet of the evaporator due to lower temperature glide. Indeed, a numerical calculation shows that at measured ammonia concentration of 96%, 80% of the refrigerant exits as vapour with a 5K glide at the evaporator outlet, while only 45% exits with a 1K glide.

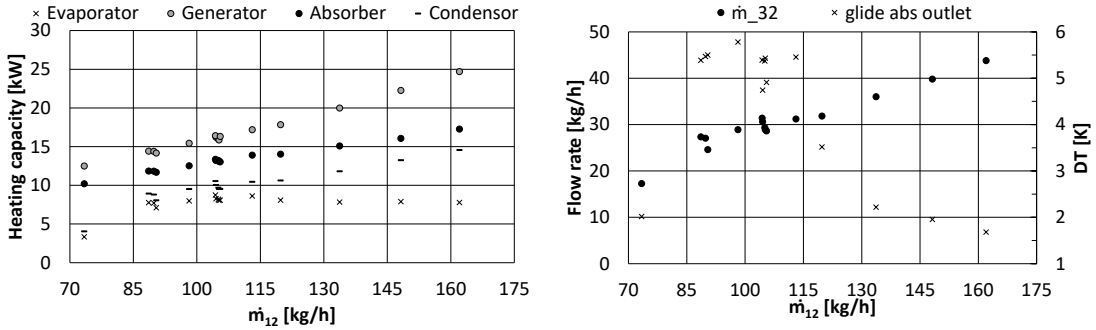

(a) Heating capacity

(b) Mass flow of the refrigerant flow and the temperature glide

Figure 7: Rich solution flow variation impact on different parameters with $T_{g,in}$=169.8°C, $T_{a,in}$=29.4°C, $T_{e,in}$= 34.5°C

- Generator temperature variation

The inlet temperature of the hot fluid at the generator is a relevant parameter because a flexibility in this sense would allow an easier management of the energy source and an increased working period. For a given solution flowrate, absorber temperature and evaporator temperature, Figure 8(a) shows a COP increase with the generator temperature. This is in line with the observations about ammonia concentration in the solution. Indeed, increasing the temperature lead to increases in the capacities of absorption and desorption represented

by $DX_{abs}=X_{12}-X_{24}$ and $DX_{des}=X_{12}-X_{22}$. In the order of magnitude, the heat production in the absorber and condenser is linked to DX_{abs} while the heat consumption in the generator is linked to DX_{des}. Therefore, the ratio between DX_{abs} and DX_{des} would represent the performance. As shown in Figure 8(b), its tendency with the generator temperature is in agreement with that of the COP.

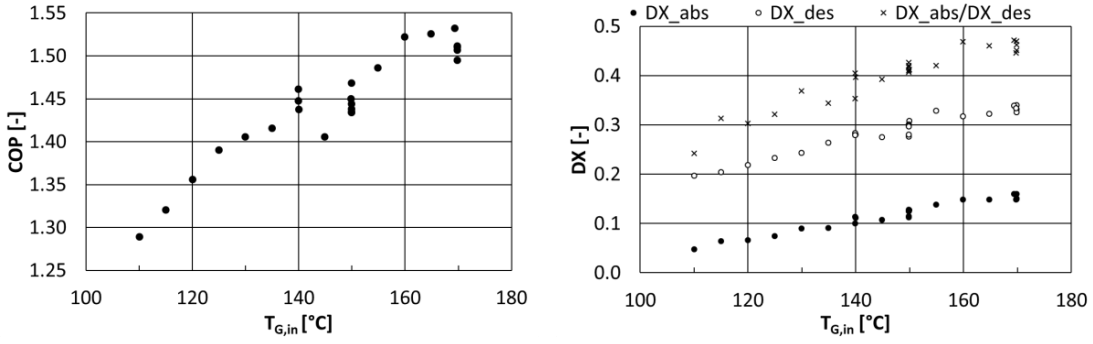

(a) COP (b) DX

Figure 8: Generator temperature variation impact on different parameters with Ta,in=29.4°C, Te,in=34.6°C, MSR=106 kg/h

The inlet evaporator temperature is representative of the low-temperature source that feeds the cycle. However, it is not necessary the ambient that would provide the input heat: for example, low-temperature waste heat could be used for this task, with positive effects on the cycle performances.

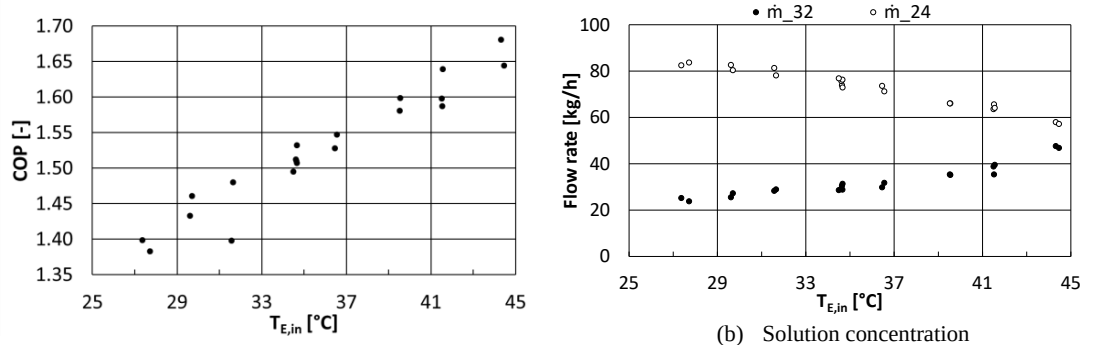

(a) COP (b) Solution concentration

Figure 9: Evaporator temperature variation impact on different parameters with $T_{a,in}$=29.4°C, $T_{g,in}$=169.8°C, M_{SR}=106kg/h

According to the expectations, increasing $T_{e,in}$ leads to a better COP, as illustrated in Figure 9(a). In particular, if the refrigerant evaporation can occur at higher temperatures, then higher pressures are allowed in the low-pressure side of the system. Operating at higher pressure is advantageous for the absorption reaction, as the equilibrium ammonia fraction of the rich solution increases with the pressure. As a result, the vapour generation flow rate ($\dot{m}_{32}$) increases with the evaporator temperature (while the poor solution mass flow rate $\dot{m}_{24}$ decreases due to a fixed pump flow rate), as shown in Figure 9(b), leading to higher COP.

6. Conclusions

This paper presents a new architecture GAX NH_3-H_2O absorption heat pump designed with plate heat exchangers in order to offer a compact machine easy-to-manufacture. An innovative architecture has been proposed with the particularity of using an internal heat exchanger (GAX1) at two level of pressure: in one side, absorption occurs at low pressure and the heat produced is transferred to other side where the desorption at high pressure can be initiated. The desorption process is internally carried out by heat recovery in the rectifier and the solution heat exchanger (GAX2). A model has been developed for design and performance simulations. Based on the numerical results, a prototype has been built with a production target of 25 kW of hot water (> 60°C) from a lower-temperature heat source of around 30°C. At nominal conditions ($T_{e,in}/T_{a,in}/T_{g,in}$)=(35/30/170)°C, the machine produces has a thermal coefficient of performance (COP) of 1.52

and an electrical coefficient of performance (ECOP) of 130. In favourable conditions, the maximum COP and power output are 1.72 and 32 kW, respectively. The tests show the capacity of the machine to operate in a wide range, especially in term of the inlet temperature of the heat source from 110°C to 170°C, with average performances in line with level of the literature. However, the experimental COPs are 10% lower than the simulated values. This might be due to different reasons: such as an improper configuration of the absorber and a limited control of the rectification in some operating conditions. These observations will be taken into account for further improvement of the prototype.

7. Declaration of Competing Interest

The authors declare that they have no known competing financial interests or personal relationships that could have appeared to influence the work reported in this paper.

8. Acknowledgements

The authors would like to express their gratitude to the French Alternative Energies and Atomic Energy Commission and the Auvergne-Rhône-Alpes region for the financial support.

9. References

Aprile M., Scoccia R., Toppi T., Guerra M. & Motta M. Modelling and experimental analysis of a GAX NH3-H2O gas-driven absorption heat pump. International journal of refrigeration, Vol. 66, pp. 155-155, 2016.

Aste F., Phan H.T., Numerical Study on Multi-effect and Multi-stage NH3/H2O Absorption Chillers for Negative Cooling in SHIP Systems, SolarPACES 2021 Conference Proceedings, 2022.

Boudehenn F., Bonnot S., Demasles H.& Lazrak A., Comparison of different modeling methods for a single effect water-lithium bromide absorption chiller. EuroSun 2014 Conference Proceedings, 2014.

Dai E., Lin M., Xia J. & Dai Y. Experimental investigation on a GAX based absorption heat pump driven by hybrid liquefied petroleum gas and solar energy. Solar Energy, Vol. 169, pp. 167-178, 2018.

Herold K. E., Radermacher R. & Klein S. A. Absorption Chillers and Heat Pumps. CRC Press, 1996.

Ibrahim O.M. and Klein S.A. Thermodynamic Properties of Ammonia-Water Mixtures. ASHRAE Trans.: Symposia, Vol. 21 (2), pp. 1495-1502, 1993.

Sun J., Fu L. & Zhang S. A review of working fluis of absorption cycles. Renewable and sustainable energy review, Vol. 16, pp. 1899-1906, 2012.

Wang J., Wu W., Shi W., Li X. & Wang B. Experimental investigation on NH3-H2O generator-absorber heat exchange (GAX) absorption heat pump. Energy, Vol. 185, pp. 337-349, 2019.

Wirtz M., Stutz B., Phan H.T. & Boudehenn F., Numerical modeling of falling-film plate generator and rectifier designed for NH3-H2O absorption machines. Heat and Mass Transfer, Vol. 58, pp. 431-446, 2021.